ACS Photonics

Article

pubs.acs.org/journal/apchd5

Bolometric Properties of Semiconducting and Metallic Single-Walled Carbon Nanotube Composite Films

Trevor J. Simmons,[†,‡] Gustavo Vera-Reveles,[‡,§] Gabriel González,[‡,∥] José Manuel Gutiérrez-Hernández,[‡] Robert J. Linhardt,[⊥,#,○,□,△] Hugo Navarro-Contreras,[‡] and Francisco J. González*[,‡]

[†]Center for Future Energy Systems, [⊥]Department of Chemistry and Chemical Biology, [#]Center for Biotechnology and Interdisciplinary Studies, [○]Department of Chemical and Biological Engineering, [□]Department of Biomedical Engineering, and [△]Department of Biology, Rensselaer Polytechnic Institute, 110 Eighth Street, Troy, New York 12180, United States

[‡]Coordinación para la Innovación y la Aplicación de la Ciencia y la Tecnología, Universidad Autónoma de San Luis Potosí, San Luis Potosí 78000, México

[§]Departamento de Ciencias Básicas, Instituto Tecnológico de San Luis Potosí, Soledad de Graciano Sánchez, 78437 México

[∥]Cátedras CONACYT/Universidad Autónoma de San Luis Potosí, San Luis Potosí 78000, México

Supporting Information

ABSTRACT: Single-walled carbon nanotubes (SWNTs) have shown interesting bolometric properties, making them good candidates for the detection of infrared and terahertz radiation. However, little has been reported on the bolometric characteristics of SWNT as a function of their chirality or the possible influence of composite morphology on these properties. The separation of SWNTs based on chirality allows for almost purely semiconductive or metallic SWNTs to be studied. The current study focuses on the bolometric performance of self-assembled composite films of SWNTs. The dependence of these properties on the chirality of the SWNTs was evaluated. To this end, metallic, semiconducting, and a 1:1 mixture of metallic and semiconductive were studied. Also, a theoretical model based on the Wiedemann−Franz law is used to explain the resistance of the SWNT composite films as a function of temperature. Results show that the composite morphology has a significant impact on bolometer performance, with cracked composite films containing highly aligned SWNT arrays suspended over a silicon substrate showing superior responsivity values due to higher thermal isolation. Uncracked composite films showed superior thermal coefficient of resistance values (α = −6.5%/K), however, the responsivity was lower due to lower thermal isolation.

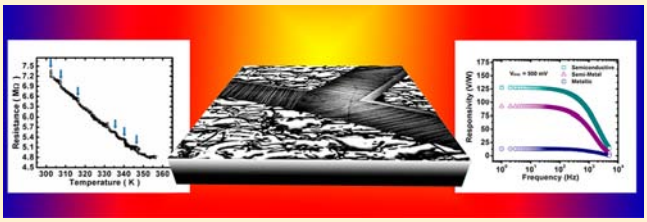

KEYWORDS: *bolometer, carbon nanotube, chirality, composite, infrared detector*

Carbon nanotubes (CNTs) are cylindrical tubes of sp^2-hybridized carbon. These structures have been studied extensively over the past two decades and continue to find new applications. The optoelectronic properties of single-walled carbon nanotubes (SWNTs) make them an attractive candidate for infrared sensors.[1−3] Uncooled microbolometers, which are a specific class of infrared detectors,[4] represent a promising application for SWNTs. Previous work has shown that self-assembled arrays of highly aligned SWNTs in a polymer−surfactant matrix can achieve bolometric properties superior to those reported in prior CNT-bolometer studies.[5] The current work evaluates how the SWNT composite morphology along with intrinsic SWNT properties affect the performance of these microbolometer devices.

Single-walled carbon nanotubes (SWNTs) may exist as either metallic or semiconductive, depending on their chirality, and in general, the bulk synthesis of SWNTs results in one-third having metallic character and two-thirds having semiconductive character.[6,7] Recent advances in CNT processing have allowed for the separation of these nanotubes based on chirality.[8] These nanotube separations exhibit almost purely semiconductive or metallic properties, depending on the sample preparation, and have recently become commercially available.

Microbolometers are devices that can detect infrared radiation through a change in their electrical resistance. When the bolometer material absorbs infrared radiation, its temperature increases, and there is a commensurate change in the electrical resistance known as the temperature coefficient of resistance (TCR or α), which is measured in percent change of resistance per degree Kelvin (%/K). In the case of semiconductors, increasing temperature due to incident infrared radiation will promote valence electrons into the conduction band, thus, reducing the electrical resistance of the material. In the case of metals, increasing temperature due to incident infrared radiation will increase the electrical resistance of the material. The conversion of incident radiation to electrical signals is known as the responsivity (R_v) and is measured in

Received: August 5, 2014
Published: January 28, 2015

   DOI: 10.1021/ph500285r

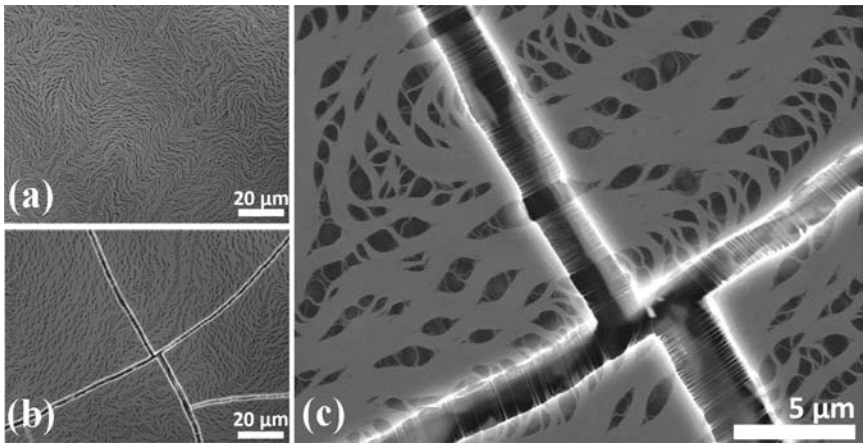

Figure 1. SEM images of an uncracked film (a) and cracked film (b), with higher magnification (c), showing the SWNTs are aligned perpendicular to the cracks and suspended above the substrate.

volts per watt (V/W). These two key figures of merit, TCR and R_v, were evaluated in the current study.

The influence of the self-assembled film architecture on bolometric performance was evaluated by creating composite films with or without large cracks that create arrays of suspended aligned SWNTs. Self-assembled composite films of two distinct types of SWNTs, metallic and semiconductive, were also studied to determine their suitability for use in uncooled microbolometer applications.

The SWNT composite films studied exhibit exceptional bolometric properties,[5] and can outperform a variety of bolometers including those based on carbon nanotubes.[4,9−12]

EXPERIMENTAL METHODS

As-produced single-walled carbon nanotubes were purchased from Swan Chemical Inc. (Elicarb SW, wet cake). Enriched chirality SWNTs were purchased from NanoIntegris (IsoNanotubes-S (semiconductive) and IsoNanotubes-M (metallic), powder, 95% chirality enriched, <1% metal catalyst, 1−5% amorphous carbon). The polymer polyvinylpyrrolidone (PVP, 10 kDa) and the surfactant sodium dodecylbenzenesulfonate (SDBS) were purchased from Sigma-Aldrich. The detailed sample preparation and device fabrication are described elsewhere.[5,13,14] Briefly, the SWNTs were combined with SDBS and bath sonicated, then PVP is added and further sonication is applied. The resultant ink is dried horizontal on a polished silica substrate in either a dry (<15% relative humidity) or humid environment (>80% relative humidity) at 80 °C for several hours. The dry environment results in a film being deposited with numerous large micron-scale cracks. The cracks in the dried composite contain highly aligned SWNTs suspended above the substrate perpendicular to the crack. In contrast, the humid environment prevents the formation of such cracks, and although the SWNTs form large aligned bundles in these composites, the samples do not exhibit suspended arrays of SWNTs. The dried composites are comprised of 6.25 wt % SWNTs, 31.25 wt % SDBS, and 62.50 wt % PVP. The film thickness was approximately 2 μm. Copper electrodes are attached with silver paint on both sides of the film surface. As-produced SWNTs (Elicarb-SW) were used in the composite film morphology studies. IsoNanotubes-S (95% semiconductive), IsoNanotubes-M (95% metallic), and with a 1:1 mixture of IsoNanotubes-S with IsoNanotubes-M (semi-metal) were used to study the effect of SWNT chirality on bolometric proerties. The absorption spectra of these nanotubes, as provided by the manufacturer, is included in the Supporting Information.

The temperature coefficient of resistance (denoted as TCR or simply α) was calculated from the resistance and temperature of samples as recorded by two independent Fluke 289 digital multimeters connected to a laptop computer. Temperature was determined with a type K thermocouple while heating the SWNT film from below with a Peltier thermoelectric device. The experimental TCR was calculated from relationship 1:[15]

$$\mathrm{TCR} = \frac{1}{R}\frac{\mathrm{d}R}{\mathrm{d}T} \tag{1}$$

Thermal time constant (τ) values were calculated by applying a voltage pulse train to the SWNT device through a load resistor with a function generator while monitoring the current response of the SWNT device with a digital oscilloscope.[4] Thermal time constants were calculated at the point when the voltage reached 63% of its stationary current value.[16]

The current−voltage (I−V) properties were measured at atmospheric pressure and temperature, both in dark and illuminated conditions with a Keithley 617 electrometer. The applied voltage was varied from 0.10 to 0.50 V, and the voltage responsivity $\mathcal{R}_V$ was calculated as a function of the applied voltage (relationship 2).[5,17]

$$\mathcal{R}_V = \frac{\Delta_V}{P_{inc}} \tag{2}$$

P_{inc} is the optical power incident on the bolometer, which in the current work is the integral of the power emitted by the tungsten-halogen lamp from 300 nm to 2 μm. The difference in output voltage given by the bolometer due to the change in resistance resulting from the heating of the bolometer by the tungsten-halogen lamp is given as Δ_V. The light source used was a tungsten-halogen lamp (Ocean Optics LS-1, 3100 K, spectral emission range 300 nm to 2 μm), with an emitted power of 0.48 mW over its entire spectral range. This lamp's peak power was at 700−950 nm, and then drops off in power significantly above 1850 nm. The nanotubes studied have their peak optical absorbance at approximately 700 nm for metallic and 900 nm for semiconducting, which means that the heat generated in these samples from the lamp used will be essentially equal. It should be noted that bolometer perform-

ance is theoretically flat over all wavelengths, and although bolometer applications are typically in the IR range, preliminary studies in the visible range can accurately predict performance in the infrared.[18]

Responsivity is calculated by the following relationship:[19]

$$\mathcal{R}_V = \alpha |Z_{th}| V_{bias} \quad (3)$$

The temperature coefficient of resistance of the bolometer is given as α, V_{bias} is the DC bias voltage across the device, and Z_{th} is the thermal impedance of the device. The relationship 3 shows that the responsivity ($\mathcal{R}_V$) is directly proportional to the temperature coefficient of resistance (α) and to the thermal impedance (Z_{th}). Thermal conductivity (G_{th}) is the main heat loss mechanism and is given by Z_{th}^{-1}. In the case of resistive bolometers, the thermal isolation has a bigger impact on responsivity than the choice of bolometric material.[20] The main heat conduction paths out of a bolometer are through its electrical contacts and through the supporting substrate, responsivity can be greatly enhanced if these heat conduction paths are reduced or eliminated. The most common measures to reduce the heat conduction paths involve suspending the devices in air,[21] which is the case in the cracked SWNT composite films studied herein.

RESULTS AND DISCUSSION

Effect of Morphology. The deposition of the SWNT composite from solution was carried out in a conventional lab oven. The relative humidity in the oven had a strong influence over the SWNT composite. When the drying process occurs rapidly in low humidity, the composite formed of exhibits micron-scale cracks throughout. However, when the humidity is high and the drying occurs slower, very few if any cracks are observed. Relative humidity of approximately 80% during deposition results in uniform composites with minimal cracking (Figure 1a). Low relative humidity of approximately 20% during the deposition process results composites with a large number of cracks (Figure 1b,c). To examine the effect of these features, as-produced SWNTs (a mixture of semiconducting and metallic) were used.

TCR measurements of the composites showed higher values at room temperature for uncracked films (α = −6.5%/K ± 2.9%/K) relative to cracked films (α = −3.8%/K ± 1.2%/K). The variation in the TCR values for uncracked films is more than twice what was recorded for the cracked composites. The reduced variability of the TCR values in the measurement of the cracked films is likely a result of the improved thermal insulation of the SWNTs from the substrate by being suspended across the cracks.[22] This is also reflected in the thermal impedance shown in Table 1.

Suspended nanotube bundles (Figure 1c) generated during the drying process of cracked films are likely responsible for the greater $\mathcal{R}_V$ values and the substantial difference in the Z_{th} values observed. This thermal isolation of the SWNTs increases the response of these devices. Uncracked film responsivity was 51.0 V/W (V_{bias} = 500 mV) and cracked film responsivity was 62.5 V/W (V_{bias} = 500 mV; Figure 2).

Table 1. Experimental Thermal Impedance (Z_{th}) and Thermal Conductance (G_{th}) Values of Cracked and Uncracked SWNT Composite Films for Temperatures of 300−302 K (As-Produced SWNTs Were Used)

	$\mathcal{R}_V$ (V/W)	α (%K^{-1})	V_{bias} (V)	Z_{th} (K/W)	G_{th} (W/K)
cracked	62.5	−3.76	0.5	3324.5	3.0e−4
uncracked	51.0	−6.5	0.5	1569.2	6.4e−4

The time constant (τ) for the uncracked and cracked composite films was at 63% of maximum response was approximately 200 μs. This is impressive when considering that vanadium oxide bolometers typically have time constants in the millisecond range.[17] While the cracked films do exhibit a greater responsivity due to higher thermal isolation, the TCR of the CNT films remains the key figure of merit. Since several methods to increase thermal isolation could be employed to increase the responsivity of uncracked films, and since the cracks of the cracked films appear at random, uncracked films seem to have greater promise for bolometric applications. The higher absolute TCR value of uncracked samples may be due to increased alignment and continuity of the nanotube bundles throughout the sample, whereas in the case of the cracked films the continuity of the film is reduced. Based on the fact that the key figure of merit was higher for the uncracked films, subsequent studies presented herein were carried out with uncracked SWNT films.

Effect of SWNT Chirality. Composite films containing semiconductive, metallic, and a mixture of metallic and semiconductive (semi-metal) SWNTs were deposited in a humid environment to prevent cracks as previously described. The conductivity of these films was 0.9 × 10^{-8} S m^{-1} for semiconductive, 2.1 × 10^{-8} S m^{-1} for metallic, and 1.9 × 10^{-8} S m^{-1} for the semi-metal sample. The time constants were τ = 440 μs for the semiconductive samples and τ = 560 μs for both the metallic and the semi-metal samples (Figure 3); therefore, the responsivity values were measured at 1.79 and 2.27 kHz, respectively.

The semiconductive SWNT composite exhibited the largest TCR values (α = −6.5%/K), these SWNTs also exhibited the largest variation of ±1.9%/K. The semiconductive SWNTs also exhibited the highest responsivity values of approximately 125 V/W (V_{bias} = 500 mV; Figure 4). The metallic SWNTs exhibited substantially smaller TCR values (α = −2.3%/K, ± 0.9%/K). The 1:1 mixture of these two types of SWNT exhibited moderately improved TCR values (α = −3.0%/K) while exhibiting the lowest variability (± 0.4%/K).

True metals will have a positive TCR value, but the metallic SWNTs studied exhibited a negative TCR. This can be explained both by the fact that the SWNTs have only been enriched to 95% metallic and that metallic SWNTs only exhibit true metallic behavior when isolated into individual SWNTs. When metallic SWNTs are in bundles, as they are in the current study, they exhibit semiconducting behavior due to interactions between the tubes.[23]

The semi-metal mixture exhibited a responsivity of 93 V/W at V_{bias} = 500 mV. When considering the values obtained for purely semiconductive and metallic SWNTs, the predicted value for this 1:1 mixture should be approximately 71 V/W. This larger observed value for the responsivity of the 1:1 mixture is possibly due to the combination of the desirable bolometric properties of the semiconductive SWNTs with the desirable conductivity of the metallic SWNTs, resulting in an advantageous synergy (Table 2).

Recently it was reported[12] that enriched chirality semiconductive SWNTs combined with the conductive polymer P3HT can marginally outperform bolometers made from standard mixed chirality SWNTs with the nonconductive polymer PVP.[5] While it is clear from the results shown in Table

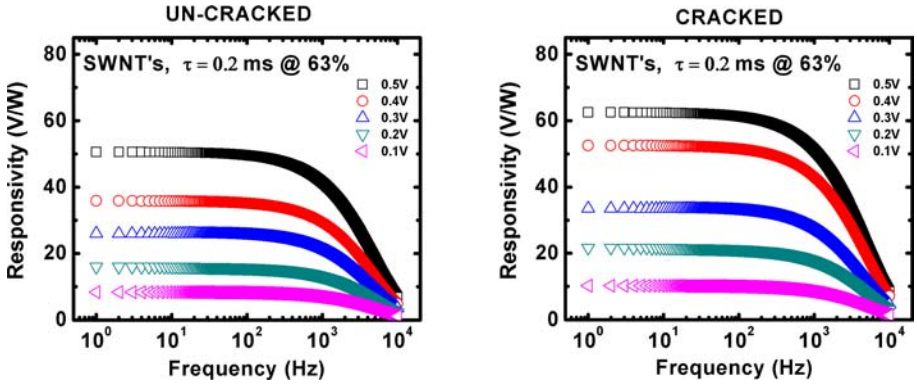

Figure 2. Responsivity curves for uncracked and cracked samples biased over a range from 100 to 500 mV (as-produced SWNTs were used).

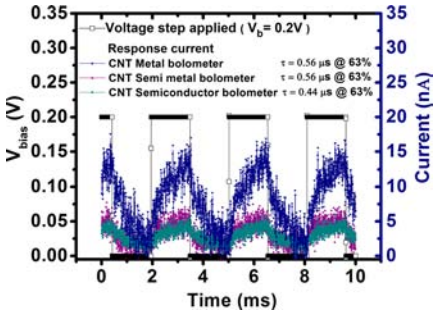

Figure 3. Response time of the three SWNT samples studied: metallic, semi-metal mixture, and semiconductive. The time constants shown were used to determine the frequency for the responsivity to measured, which was 2.27 kHz for metallic SWNTs and the semi-metal mixture, and 1.79 kHz for semiconductive SWNTs.

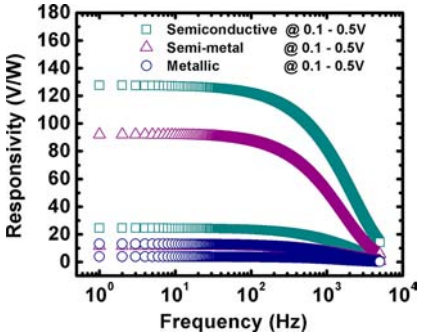

Figure 4. Responsivity of composite bolometers containing semiconductive (□), metallic (○), and a semi-metal mixture (Δ) of SWNTs at V_{bias} = 100 mV (lower curves) and V_{bias} = 500 mV (upper curves).

Table 2. Responsivity Shown is Based on Achieving 63% Maximum Current, at a Frequency of (a) 1.79 kHz for the Semiconductive SWNT Composite Device and (b) 2.27 kHz for the Semi-Metal and Metallic SWNT Composite Devices

	responsivity, $\mathcal{R}_V$ (V/W)		
V_{bias} (mV)	semiconductive[a]	semi-metal[b]	metallic[b]
100	25	12	3.9
200	52	29	5.4
300	79	46	7.3
400	97	67	10
500	128	93	14

2 that semiconductive SWNTs have superior performance, the mixed chirality nanotubes provide impressive results. The performance of the mixtures of SWNTs reported here and elsewhere have similar bolometric properties such as TCR and R_v, and less variability than the enriched chirality semiconductive SWNTs. As enriched chirality semiconductive SWNTs become more readily available, these performance trade-offs should be considered.

Wiedemann–Franz Law in Bolometric SWNT Composite Films. In an effort to better understand the bolometric response of the SWNT composite materials studied and to move beyond the experimental TCR values obtained, a theoretical model was applied to the experimental data. Figure 5 shows the temperature dependence of the resistance of a mixture of metallic and semiconductive SWNTs in a bolometric composite film as a function of temperature. It is worth noting that this curve shows spikes that appear at the moment when the temperature of the Peltier heating unit is increased, and these spikes in resistance are explained in terms of the Wiedemann–Franz law.

Typically when a material is heated by the absorbance of infrared radiation, the resistivity either increases or decreases. When the temperature range is not large and near room temperature, the following linear approximation may be used (relationship 4):

$$\rho(T) = \rho_0[1 + \alpha\Delta T] \tag{4}$$

where resistivity (ρ) for a given temperature (T) is defined by an experimental thermal coefficient (α), the initial resistivity (ρ_0), and the change from the temperature (ΔT).

In metals, the resistivity increases with increasing temperature due to electron–phonon interactions arising from the increased thermal energy. Semiconductors will exhibit reduced resistivity with increasing temperature as electrons are excited to the conduction band by the increased thermal energy. The resistivity of an intrinsic semiconductor will decrease exponentially with temperature following the exponential relationship 5:

$$\rho = \rho_0 e^{-\alpha T} \tag{5}$$

where the resistivity (ρ) for a given temperature (T) is defined by an experimental thermal coefficient (α), the initial resistivity (ρ_0).

It follows from Figure 5 that there is an intrinsic response from the CNT associated with the temperature gradient which induces an increase in the TCR values. Our starting point to account for these results is the heat conduction relationship 6:

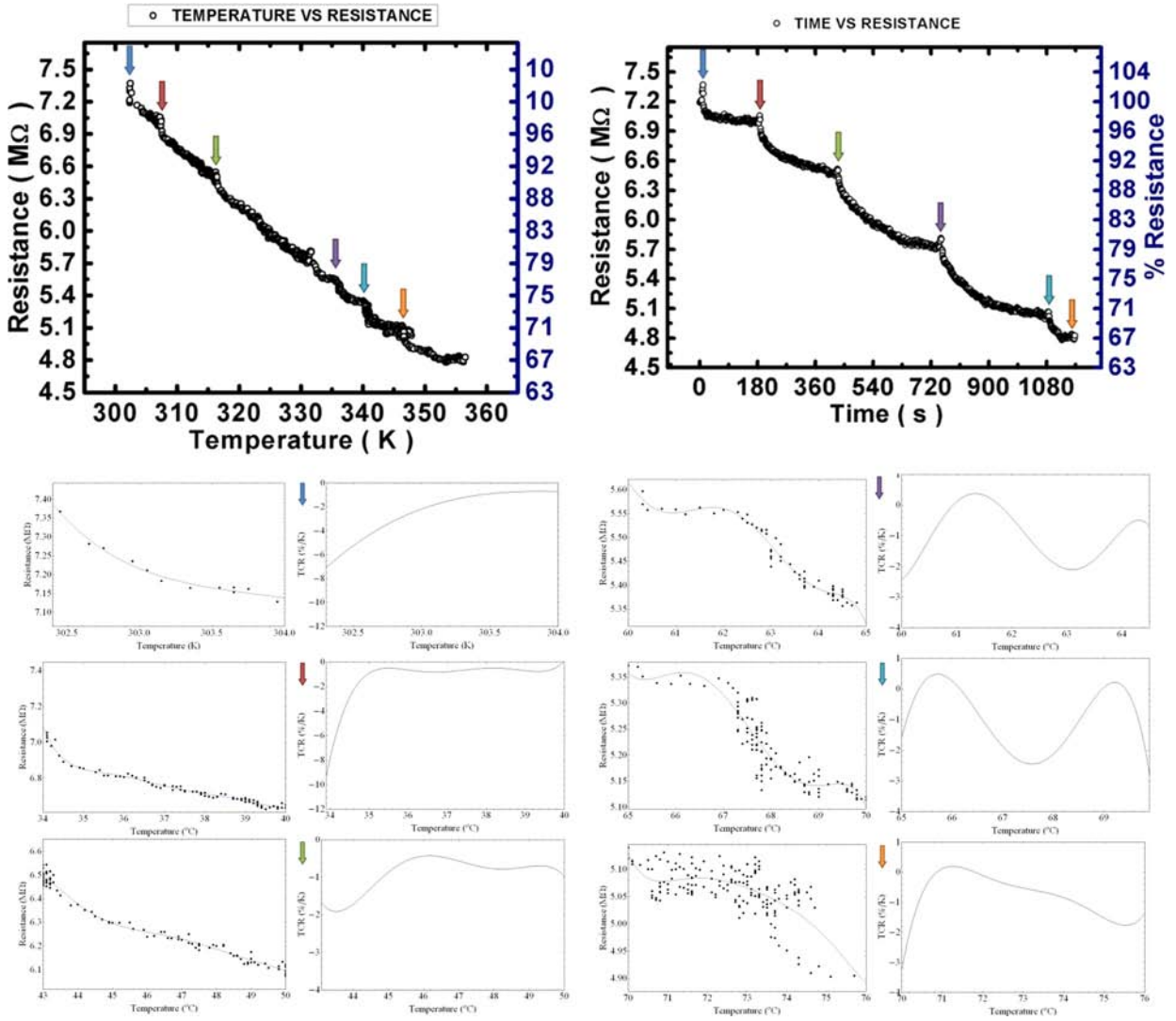

Figure 5. Resistance as a function of temperature (left) and as a function of time (right) for uncracked composite films of semi-metal SWNTs. Colored arrows indicate the location of spikes where the Peltier heating device increased its temperature. The fit of the experimental data points to the theoretical predictions for the six observed spikes is shown below each graph.

$$\frac{\Delta Q}{\Delta t} = -\kappa A \frac{\Delta T}{\Delta x} \tag{6}$$

where $\Delta Q/\Delta t$ is the heat production per time, κ is the thermal conductivity, A is the cross sectional area, and $\Delta T/\Delta x$ represents the temperature gradient. The thermal gradient being from the surface of the substrate to the top of the SWNT composite film, normal to the substrate. Using the Wiedemann−Franz law, which states that the thermal conductivity κ and the electrical conductivity σ of a metal is proportional to the temperature by $\kappa = \sigma LT$, where $L = 2.44 \times 10^{-8} W\Omega/K^2$ is the so-called Lorenz number, we have relationship 7:

$$\frac{1}{\sigma} = \rho = \frac{LTA}{-(\Delta Q/\Delta t)} \frac{\Delta T}{\Delta x} \tag{7}$$

Using the fact that $\rho = (A/l)R$, where l and R are the length of the conductor and electrical resistance, respectively, we have the following relation 8 between the temperature gradient normal to the substrate and resistance:

$$R = \frac{LTl}{-(\Delta Q/\Delta t)} \frac{\Delta T}{\Delta x} \tag{8}$$

Integrating the above relation, we obtain the average electrical resistance as a function of the temperature (relationship 9), where $T_1 > T_2$.

$$\begin{aligned} \langle R \rangle &= \frac{1}{l} \int_0^l R \mathrm{d}x \\ &= \frac{-L}{(\Delta Q/\Delta t)} \int_{T_1}^{T_2} T \frac{\Delta T}{\Delta x} \mathrm{d}x \\ &= \frac{L}{(\Delta Q/\Delta t)} \left(\frac{T_1^2}{2} - \frac{T_2^2}{2} \right) \end{aligned} \tag{9}$$

Using the above equation and the measurements for the electrical resistance as a function of temperature depicted in Figure 5, we obtained the rate of heat flow for each spike depicted in the above figures, which are listed in the table below. It is worth noting that the rate of heat flow is minimal for the first spike and is approximately equal to the rest of the spikes for the same temperature gradient. This indicates that

Table 3. Calculated Values for TCR Based on Theoretical Considerations Derived from the Wiedemann−Franz Law at Various Temperatures

calculated TCR using Wiedemann−Franz law					
spike	T_1 (K)	T_2 (K)	R (Ω)	Q/T (W)	TCR (%·K^{-1})
1	302.35	302.45	1.53×10^5	-4.8×10^{-12}	−9.5
2	307.25	307.35	5.7×10^4	-1.31×10^{-11}	−2.0
3	316.25	316.35	6.2×10^4	-1.25×10^{-11}	−2.4
4	331.35	331.45	6.2×10^4	-1.30×10^{-11}	−2.4
5	346.65	346.74	6.7×10^4	-1.14×10^{-11}	−3.0

the average resistance is at a maximum in the first spike and essentially the same for subsequent spikes, which agrees with the TCR measurements obtained by applying eq 1 to the values obtained experimentally and shown in Figure 5.

The Wiedemann−Franz law applies for single carrier processes, and the heat conducted by electrons accounts for less than 15% of the heat conduction in carbon nanotubes,[24] however, due to the close fit of our model to the experimental data we propose a Weidemann−Franz-like behavior (Table 3). Further experiments are underway to determine a physical model not restricted by single carrier physics.

CONCLUSIONS

This work has shown that both composite morphology and carbon nanotube chirality play important roles in bolometer performance. SWNT composite films with a large amount of SWNTs suspended across cracks in the composite exhibit higher responsivity but with reduced absolute TCR values. This a result of their increased thermal impedance. Uncracked SWNT composite films yielded somewhat lower responsivity but showed the highest absolute TCR values. A theoretical model based on the Wiedemann−Franz law that explains the abrupt changes in resistance due to changes in temperature for a composite film of semiconductive SWNTs has been developed that may help in the design of bolometers based on SWNT composite films.

It is worth noting that the presence of suspended aligned arrays of SWNTs creates structures similar to MEMS fabricated microbolometers, with the IR absorbing material thermally isolated and suspended above a silicon substrate. Further studies will be required to fully understand how the composite matrix can be tailored to meet performance requirements. Enriched chirality semiconductive SWNTs exhibited superior bolometric properties compared to enriched chirality metallic SWNTs or a mixture of these two chiralities. Surprisingly, however, a mixture of metallic and semiconductive SWNTs performed admirably, suggesting that the heterogeneous mixture of chiralities found in as-produced SWNTs may be suitable for high-performance bolometer applications.

ASSOCIATED CONTENT

Supporting Information

Supporting figure (Figure S1). This material is available free of charge via the Internet at http://pubs.acs.org.

AUTHOR INFORMATION

Corresponding Author

*E-mail: javier.gonzalez@uaslp.mx. Tel.: +52 (444) 826-2300, ext 8416.

Notes

The authors declare no competing financial interest.

ACKNOWLEDGMENTS

This work was supported by the project "Centro Mexicano de Innovación en Energía Solar" from Fondo Sectorial CONACYT-Secretaría de Energía-Sustentabilidad Energética" and through the program "Cátedras CONACYT".

REFERENCES

(1) Xu, J. M. Highly ordered carbon nanotube arrays and IR detection. *Infrared Phys. Technol.* **2001**, *42*, 485−491.
(2) Wildoer, J. W. G.; Venema, L. C.; Rinzler, A. G.; Smalley, R. E.; Dekker, C. Electronic structure of atomically resolved carbon nanotubes. *Nature* **1998**, *391*, 59−62.
(3) Odom, T. W.; Huang, J.; Kim, P.; Lieber, C. M. Atomic structure and electronic properties of single-walled carbon nanotubes. *Nature* **1998**, *391*, 62−64.
(4) Itkis, M. E.; Borondics, F.; Yu, A.; Haddon, R. C. Bolometric infrared photoresponse of suspended single-walled carbon nanotube films. *Science* **2006**, *312*, 413−416.
(5) Vera-Reveles, G.; Simmons, T. J.; Bravo-Sanchez, M.; Vidal, M. A.; Navarro-Contreras, H.; Gonzalez, F. J. High-sensitivity bolometers from self-oriented single-walled carbon nanotube composites. *ACS Appl. Mater. Interfaces* **2011**, *3*, 3200−3204.
(6) Dresselhaus, M. S.; Dresselhaus, G.; Saito, R.; Jorio, A. Raman spectroscopy of carbon nanotubes. *Phys. Rep* **2005**, *409*, 47.
(7) Zhao, Y.; Nakano, H.; Murakami, H.; Sugai, T.; Shinohara, H.; Saito, Y. Controllable growth and characterization of isolated single-walled carbon nanotubes catalyzed by Co particles. *Appl. Phys. A: Mater. Sci. Process.* **2006**, *85*, 103−107.
(8) Ghosh, S.; Bachilo, S. M.; Weisman, R. B. Advanced sorting of single-walled carbon nanotubes by nonlinear density-gradient ultracentrifugation. *Nat. Nanotechnol.* **2010**, *5*, 443−450.
(9) Lu, R.; Li, Z.; Xu, G.; Wu, J. Z. Suspending single-wall carbon nanotube thin film infrared bolometers on microchannels. *Appl. Phys. Lett.* **2009**, *94*, 163110.
(10) Aliev, A. E. Bolometric detector on the basis of single-wall carbon nanotubes/polymer composite. *Infrared Phys. Technol.* **2008**, *51*, 541−545.
(11) Xiao, L.; Zhang, Y.; Wang, Y.; Liu, K.; Wang, Z.; Li, T.; Jiang, Z.; Shi, J.; Liu, L.; Li, Q. Q.; Zhao, Y.; Feng, Z.; Fan, S.; Jiang, K. A polarized infrared thermal detector made from super-aligned multi-walled carbon nanotube films. *Nanotechnology* **2011**, *22* (025502), 7.
(12) Lu, R.; Christianson, C.; Kirkeminde, A.; Ren, S.; Wu, J. Extraordinary photocurrent harvesting at type-II heterojunction interfaces: toward high detectivity carbon nanotube infrared detectors. *Nano Lett.* **2012**, *12* (12), 6244−6249.
(13) Simmons, T. J.; Hashim, D.; Vajtai, R.; Ajayan, P. M. Large area-aligned arrays from direct deposition of single-wall carbon nanotube inks. *J. Am. Chem. Soc.* **2007**, *129*, 10088−9.
(14) Bravo-Sanchez, M.; Simmons, T. J.; Vidal, M. A. Liquid crystal behavior of single wall carbon nanotubes. *Carbon* **2010**, *48*, 3531−3542.
(15) Kumar, R. T. R.; Karunagaran, B.; Mangalaraj, D.; Narayandass, S. K.; Manoravi, P.; Joseph, M.; Gopal, V. Study of a pulsed laser deposited vanadium oxide based microbolometer array. *Smart Mater. Struct.* **2003**, *12*, 188−192.

(16) Woo, C. S.; Lim, C. H.; Cho, C. W.; Park, B. H.; Ju, H. K.; Min, D. H.; Lee, C. J. Fabrication of flexible and transparent single-wall carbon nanotube gas sensors by vacuum filtration and poly(dimethyl siloxane) mold transfer. *Microelectron. Eng.* **2007**, *84*, 1610−1613.
(17) Ham, M. H.; Kong, B. S.; Kim, W. J.; Jung, H. T.; Strano, M. S. Unusually large Franz-Keldysh oscillations at ultraviolet wavelengths in single-walled carbon nanotubes. *Phys. Rev. Lett.* **2009**, *102*, 047402.
(18) Dereniak, D. L.; Boreman, G. D. *Infrared Detectors and Systems*; John Wiley & Sons: New York, 1996, Chapter 2, pp 72−76.
(19) Gonzalez, F. J.; Fumeaux, C.; Alda, J.; Boreman, G. D. Thermal impedance model of electrostatic discharge effects on microbolometers. *Microwave Opt. Technol. Lett.* **2000**, *26* (5), 291−293.
(20) Gonzalez, F. J. Antenna-coupled infrared focal plane array. *Ph.D. dissertation*, UCF, Orlando, FL, 2003.
(21) Neikirk, D. P.; Rutledge, D. B. Air-bridge microbolometer for far-infrared detection. *Appl. Phys. Lett.* **1984**, *44* (2), 153−155.
(22) Gonzalez, F. J. Thermal-impedance simulations of antenna-coupled microbolometers. *Infrared Phys. Technol.* **2006**, *48* (3), 223−226.
(23) Ouyang, M.; Huang, J. L.; Cheung, C. L.; Lieber, C. M. Energy gaps in "metallic" single-walled carbon nanotubes. *Science* **2001**, *292* (5517), 702−705.
(24) Pop, E.; Mann, D. A.; Goodson, K. E.; Dai, H. Electrical and thermal transport in metallic single-wall carbon nanotubes on insulating substrates. *J. Appl. Phys.* **2007**, *101*, 093710.